

Article

Kinetic, Isothermal, and Thermodynamic Analyses of Adsorption of Humic Acid on Quaternized Porous Cellulose Beads

Kana Uchiyama¹, Hiromichi Asamoto², Hiroaki Minamisawa² and Kazunori Yamada^{3,*} 

¹ Major of Applied Molecular Chemistry, Graduate School of Industrial Technology, Nihon University, 1-2-1 Izumi-cho, Narashino 275-8585, Chiba, Japan; cika21013@g.nihon-u.ac.jp

² Department of Basic Science, College of Industrial Technology, Nihon University, 2-11-1 Shin-ei, Narashino 275-8576, Chiba, Japan; asamoto.hiromichi@nihon-u.ac.jp (H.A.); minamisawa.hiroaki@nihon-u.ac.jp (H.M.)

³ Department of Applied Molecular Chemistry, College of Industrial Technology, Nihon University, 1-2-1 Izumi-cho, Narashino 275-8575, Chiba, Japan

* Correspondence: yamada.kazunori@nihon-u.ac.jp; Tel.: +81-47-474-2571

Abstract: Porous cellulose beads were quaternized with glycidyltrimethylammonium chloride (GTMAC), and the potential use of the quaternized cellulose beads as an adsorbent was explored for the removal of humic acid (HA) from aqueous media. The introduction of quaternary ammonium groups was verified by FT-IR and XPS analyses, and their content increased to 0.524 mmol/g-Qcell by increasing the GTMAC concentration. The adsorption capacity of the HA increased with decreasing initial pH value and/or increasing content of quaternary ammonium groups, and a maximum adsorption capacity of 575 mg/g-Qcell was obtained for the quaternized cellulose beads with a content of quaternary ammonium groups of 0.380 mmol/g-Qcell. The removal % value increased with increasing dose of quaternized cellulose beads, and HA was highly removed at higher quaternary ammonium groups. The kinetics of the HA adsorption in this study followed a pseudo-second-order equation, and the process exhibited a better fit to the Langmuir isotherm. In addition, the k_2 value increased with increasing temperature. These results emphasize that HA adsorption is limited by chemical sorption or chemisorption. The quaternized cellulose beads were repetitively used for the adsorption of HA without appreciable loss in the adsorption capacity. The empirical, equilibrium, and kinetic aspects obtained in this study support that the quaternized cellulose beads can be applied to the removal of HA.

Keywords: quaternized porous cellulose beads; humic acid; adsorption; desorption; kinetic analysis; isothermal analysis



Citation: Uchiyama, K.; Asamoto, H.; Minamisawa, H.; Yamada, K. Kinetic, Isothermal, and Thermodynamic Analyses of Adsorption of Humic Acid on Quaternized Porous Cellulose Beads. *Macromol* **2024**, *4*, 117–134. <https://doi.org/10.3390/macromol4010006>

Academic Editor: Ana María Díez-Pascual

Received: 6 January 2024

Revised: 28 February 2024

Accepted: 29 February 2024

Published: 5 March 2024



Copyright: © 2024 by the authors. Licensee MDPI, Basel, Switzerland. This article is an open access article distributed under the terms and conditions of the Creative Commons Attribution (CC BY) license (<https://creativecommons.org/licenses/by/4.0/>).

1. Introduction

Humic substances, which are the constituents of the natural decay of plant and animal residues, are divided into three different components in terms of their solubility, that is, fulvic acid (soluble at any pH value), humic acid (HA, insoluble below pH 2), and humin (insoluble in water) [1,2]. HA has diverse functional groups involving carboxy, phenolic hydroxy, quinone, and ether groups. Out of these functional groups, the carboxy and phenolic hydroxy groups are more prevalent in HA structures [3,4].

HA can facilitate the absorption of micro- and macroelements in plants to enhance plant growth [5]. However, the presence of HA in water has been of environmental concern, and the removal of HA has become a necessary procedure in the water supply for our economy and community for the following reasons [6]. First, the presence of HA causes a yellowish or brownish color, bad taste and odor, and the growth of pathogenic microorganisms. Also, HA can readily chelate with metal ions in aqueous environments [7]. Although chlorination is the most widely used technique for the disinfection of drinking

water, some of the disinfection byproducts generated by the reaction of HA with chlorine are more toxic and carcinogenic [8,9]. In addition, calcium and magnesium ions can aggravate membrane fouling due to the fact that these ions promote aggregation with HA molecules [10].

The methods for the removal of HA from aqueous media include adsorption, membrane filtration, flocculation and coagulation, and advanced oxidation processes [6,11]. One of the most prominent and most researched methods is the adsorption process. In comparison with other removal methods, the adsorption process is an effective separation technique in terms of the simplicity of the design, ease of operation, insensitiveness to other substances, and variety of target pollutants that can be removed. Activated carbons produced from different agricultural wastes have been frequently used in many studies on the adsorptive removal of HA [6,12–14]. However, some problems to be solved are raised; for example, the cost for chemical activation is high, the regeneration is difficult, the adsorption rate is low, and the adsorption capacity is low [15–17]. Therefore, their use is frequently limited. Also, in some articles, the content of the functional groups involved in adsorption was not quantitatively determined. Therefore, we focused on the development of adsorbents for HA by the chemical modification of cellulose materials in terms of the fact that cellulose does not compete with the food supply.

Cellulose is a linear polymer with repeating D-anhydro-glucopyranose units (AGUs) linked together through β -(1,4)-D-glycosidic linkages and has one primary hydroxy (-OH) group and two secondary hydroxy (-CH₂OH) groups in each AGU. Nevertheless, cellulose is insoluble in water or common organic solvents through inter- and intramolecular hydrogen-bonding interactions [18]. Based on the above points, cellulose was selected as a starting material for the ease of chemical modification through the primary and secondary hydroxy groups in this study, leading to the formation of competent functional materials as well as the abovementioned unique physicochemical properties. Indeed, many studies have been published on the application of chemically modified cellulose materials for the removal of metal ions and organic pollutants [19,20].

In this study, quaternary ammonium groups were introduced to the porous cellulose beads with glycidyltrimethylammonium chloride (GTMAC) under alkaline conditions. The introduction of the quaternary ammonium groups was verified by FT-IR and XPS analyses, and their content was determined by back titration. The adsorption behavior was estimated by varying the experimental factors, such as the initial pH value, temperature, content of quaternary ammonium groups, and dose of quaternized cellulose beads. The adsorption processes obtained were analyzed based on kinetic equations and isotherms. In addition, the HA desorption properties of the quaternized cellulose beads were estimated using different eluents for regeneration and reusability.

2. Materials and Methods

2.1. Chemicals

Porous cellulose beads, Viscopearl[®]PD-3002, were purchased from Rengo Co., Ltd. (Osaka, Japan). The characteristics of the cellulose beads are listed as follows from the nominal data: a diameter of 300 μ m, a bulk specific gravity of 0.3 g/mL, a water content of 35 w/v%, and a porosity of 87%. GTMAC was supplied as an 80 vol% solution in water from Tokyo Chemical Industry Co., Ltd. (Tokyo, Japan). Other chemicals were used without further purification.

2.2. Quaternization of Cellulose Beads

First, about 5.0 g of cellulose beads were dispersed in a NaOH solution at 5 w/v% for 24 h. Then, to this mixture, GTMAC in a NaOH solution at 5 w/v% was added [21,22] to give a GTMAC concentration of 0.10–1.0 M. The mixtures were stirred for 2 h at 65 °C. After separation by decantation, the cellulose beads were washed with ion exchange water and acetone (each several times), followed by drying under reduced pressure for 24 h [21].

2.3. Determination of Content of Quaternary Ammonium Groups

After 0.05–1.0 g of the quaternized cellulose beads were mildly stirred in 20.0 mL of a HCl solution at 10.0 mM for at least 18 h under nitrogen atmosphere, the supernatants were titrated against a NaOH solution at 10.0 mM with bromothymol blue as a pH indicator. The content of quaternary ammonium groups per 1 g of the quaternary cellulose beads was calculated from the difference in the HCl concentration using Equation (1) [21]:

$$A_{\text{quater}}^{\text{Qcell}} \text{ (mmol/g-Qcell)} = \frac{(10.0 - C_{\text{HCl}}) \cdot 0.020}{W_{\text{Qcell}}} \quad (1)$$

where C_{HCl} (mM) is the concentration of HCl solution to which the quaternized cellulose beads were added; W_{Qcell} the weight of the quaternized cellulose beads (g). The quantities of 10.0 and 0.020 are the initial concentration (mM) and volume of HCl solution (L), respectively.

In addition, the content of quaternary ammonium groups per 1 g of the original cellulose beads was determined using Equation (2):

$$A_{\text{quater}}^{\text{cell}} \text{ (mmol/g-cell)} = \frac{(10.0 - C_{\text{HCl}}) \cdot 0.020}{W_{\text{Qcell}} - W_{\text{Qcell}} \cdot A_{\text{quater}}^{\text{Qcell}} \cdot 10^{-3} \cdot (313.77 - 162.14)} \quad (2)$$

where the quantities of 162.14 and 313.77 denote the molecular mass of an untreated AGU and quaternized AGU segments, respectively.

2.4. Analysis by FT-IR and XPS

The FT-IR spectra of the untreated and quaternized cellulose beads were measured by a JASCO (Tokyo, Japan) FT/IR-4100 spectrometer. The spectra were recorded at the resolution of 4.0 cm^{-1} with 16 scans across the range of $4000\text{--}500 \text{ cm}^{-1}$. The core level spectra of C_{1s} , O_{1s} , N_{1s} , and Cl_{2p} were measured at 8 kV and 20 mA with $\text{MgK}\alpha$ radiation ($h\nu = 1253.4 \text{ eV}$) on a Shimadzu ESCA 3400 X-ray photoelectron spectrometer (Kyoto, Japan). The binding energy was calibrated with the $\text{Au}_{4f}^{7/2}$ peak at $\text{BE} = 83.8 \text{ eV}$.

2.5. Particle Distribution

The photographs (magnification of 150 times) of the untreated and quaternized cellulose beads were taken in the dry and water-swollen states using a Keyence VH-5500 microscope (Osaka, Japan) [21]. The diameters of 200 pieces of the untreated and quaternized cellulose beads were measured and the average particle size was calculated from the particle size distribution on the supposition that they were regarded as a sphere. The average particle size of quaternized cellulose beads immersed in HCl solutions at pH 3 and 6 was also determined in the same manner.

2.6. Water Content

At $25 \text{ }^\circ\text{C}$, accurately weighed 0.5 g of untreated and quaternized cellulose beads were immersed in water and in HCl solutions at pH 3 and 6 for 24 h, and the weight was measured in the water-swollen state. The water content was calculated using Equation (3):

$$\text{water content (\%)} = \frac{W_{\text{wet}} - W_{\text{dry}}}{W_{\text{wet}}} \cdot 100 \quad (3)$$

where W_{dry} and W_{wet} (g) are the weight of quaternized cellulose beads in the dry and water-swollen states, respectively.

2.7. Preparation of HA Solutions

The HA solutions were prepared according to the procedure reported in our previous article [21]. About 0.125 g of HA was dissolved in about 450 mL of water. The insoluble components were removed by filtration, and then the filtrate was made up to 500 mL with water. The concentration of the stock HA solutions was determined from the difference between the weight of added HA and the weight of insoluble residues [22]. This solution was diluted to the concentration from 40 to 175 mg/L with water, and the pH value of the HA solutions was adjusted to 3–12 with HCl or NaOH. The HA concentration was determined by the absorbance measurements. The wavelength of 254 nm as an isosbestic point with the extinction coefficient of $12.58 \text{ dm}^3/\text{g}\cdot\text{cm}$ was used in the range of pH 5–12. The extinction coefficients were 11.54 and $12.48 \text{ dm}^3/\text{g}\cdot\text{cm}$ at pH 3 and 4, respectively.

2.8. HA Adsorption

The HA adsorption experiments were performed by varying the experimental conditions, such as the initial pH, temperature, dose of quaternized cellulose beads, and content of quaternary ammonium groups in the batch method. Unless otherwise described, 10 mg of quaternized cellulose beads were added to 50 mL of a HA solution at 100 mg/L, the pH value of which was adjusted to 3.0 or 6.0 beforehand at 25 °C. The absorbance was measured until equilibrium and the adsorbed amount was calculated using Equation (4) [21,22]:

$$\text{amount of adsorbed HA, } Q_t \text{ (mg/g-Qcell)} = \frac{(C_0 - C_t) \cdot 0.050}{W_{Q_{\text{cell}}}} \quad (4)$$

where C_0 and C_t are the HA concentration (mg/L) at time 0 and t , respectively. The quantity of 0.050 denotes the volume (L) of HA solution. In addition, the removal % of HA was obtained from Equation (5) using the initial concentration and the concentration at equilibrium (C_{eq}):

$$\text{removal \%} = \frac{(C_0 - C_{\text{eq}})}{C_0} \cdot 100 \quad (5)$$

2.9. Analysis by Kinetics Equations

The kinetics of the adsorption process was analyzed by the pseudo-first-order and second-order equations shown in Equations (6) and (7), respectively [13,23,24]:

$$\ln (Q_{\text{eq}} - Q_t) = \ln Q_{\text{eq}} - k_1 t \quad (6)$$

$$\frac{t}{Q_t} = \frac{t}{k_2 \cdot Q_{\text{eq}}^2} + \frac{1}{Q_{\text{eq}}} t \quad (7)$$

where Q_{eq} denotes the adsorbed amount at equilibrium, that is, the adsorption capacity. In addition, k_1 and k_2 are the pseudo-first-order rate constant and pseudo-second-order rate constant for adsorption, respectively.

2.10. Analysis by Adsorption Isotherms

The adsorption capacity obtained at different initial HA concentrations was analyzed according to Langmuir and Freundlich isotherms shown in Equations (8) and (9), respectively [13,25,26]:

$$\frac{C_{\text{eq}}}{Q_{\text{eq}}} = \frac{1}{K_L \cdot Q_{\text{max}}} + \frac{C_{\text{eq}}}{Q_{\text{max}}} \quad (8)$$

where Q_{max} is the maximum adsorption capacity and K_L is the Langmuir adsorption constant related to the affinity of a binding site toward an adsorbate.

$$\log Q_{\text{eq}} = \log K_F + \frac{1}{n} \log C_{\text{eq}} \quad (9)$$

where K_F is the Freundlich constant related to adsorption capacity and $1/n$ is the empirical parameter related to the adsorption intensity, which varies with the heterogeneity of the material [27].

2.11. Desorption

The quaternized cellulose beads loaded with HA at pH 6 were transferred into NaOH solutions ($V = 50$ mL) at 10–200 mM at 25 °C and the absorbance at 254 nm was measured until equilibrium to calculate the desorbed amount. Desorption % was obtained by dividing the desorption amount by the adsorbed amount [21].

3. Results and Discussion

3.1. Preparation of Quaternized Cellulose

The procedure of preparation of quaternized cellulose beads with GTMAC was described in our previous article in detail [21]. Therefore, here, the results on the preparation of quaternized cellulose beads will be briefly described as follows. The content of quaternary ammonium groups increased with increasing the GTMAC concentration and increased to 0.524 mmol/g-Qcell, as shown in Figure 1. This corresponded to 0.569 mmol/g-cell, when the content of quaternary ammonium groups per 1 g of the untreated cellulose beads was calculated using Equation (2). This means that 9.23% of the AGUs were quaternized with GTMAC.

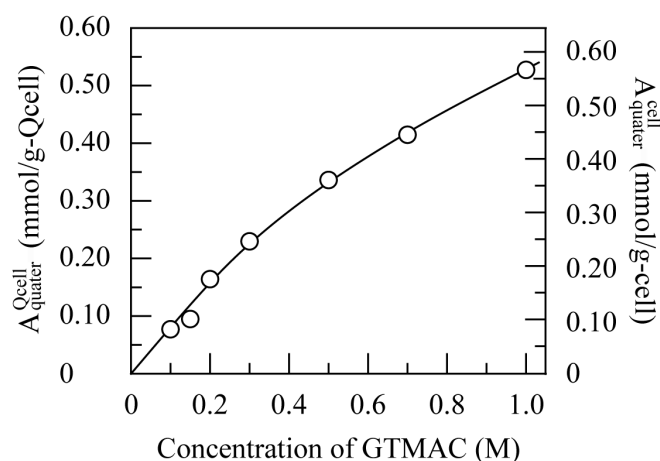
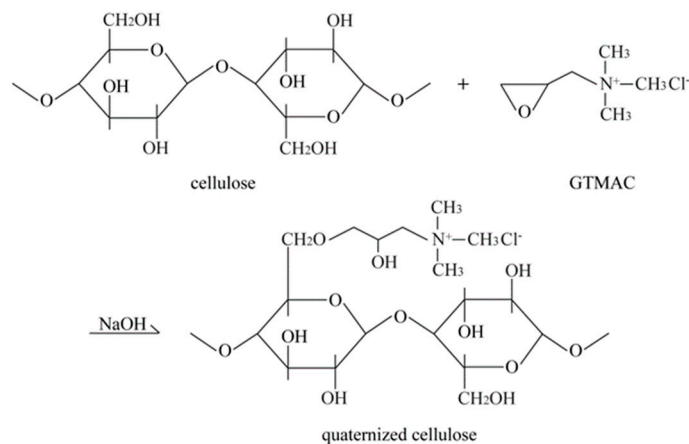


Figure 1. Change in the content of quaternary ammonium groups introduced to the cellulose beads with the concentration of GTMAC for the reaction for 2 h at 65 °C in the presence of NaOH at 5 w/v%.

The FT-IR spectra and XPS core level spectra of the untreated and quaternized cellulose beads (0.231 mmol/Q-cell) are shown in Figures S1 and S2, respectively. A specific difference between them is the appearance of two peaks at 1416 and 1476 cm^{-1} . The former corresponds to the stretching vibration of -C-N groups and the latter corresponds to the asymmetric bending of trimethyl groups of the quaternary ammonium species [22,28–30]. For the XPS analysis, a N_{1s} peak assigned to $-\text{N}^+(\text{CH}_3)_3$ groups at 402.7 eV and a Cl_{2p} peak were observed for the quaternized cellulose beads [21,30,31]. Even when treated with NaOH, the N_{1s} peak was little shifted and the Cl_{2p} peak disappeared. These instrumental results indicate that quaternary ammonium groups were successfully formed on the surfaces of the cellulose beads according to the reaction shown in Scheme 1 [21].



Scheme 1. The schematic representation of the quaternization of cellulose beads with GTMAC in the presence of NaOH.

3.2. Characterization of Quaternized Cellulose Beads

The water content was measured for quaternized cellulose beads with different contents of quaternization. As shown in Figure S3, the water content gradually increased with increase in the content of quaternary ammonium groups from 87.6% for the untreated cellulose beads and leveled off at higher than 0.25 mmol/g-Qcell. In addition, the particle size distribution is shown in Figure S4 for the quaternized cellulose beads with the quaternary ammonium groups of 0.380 mmol/g-Qcell in the dry and water-swollen states. The average particle sizes of the untreated cellulose beads were 0.298 mm (SD = 0.046 mm) and 0.395 mm (SD = 0.047 mm) in the dry and water-swollen states, respectively. As shown in Table S1, the average particle size remained unchanged, even when the content of quaternary ammonium groups increased.

3.3. HA Adsorption

3.3.1. Effect of pH

The effect of the pH value on the adsorption capacity and removal % was estimated for quaternized cellulose beads with the quaternary ammonium groups from 0.053 to 0.524 mmol/g-Qcell. As shown in Figure 2, the adsorption capacity decreased with an increase in the pH value from the maximum value at 3.0, with a sharp decrease at around pH 3.5–5 for the quaternized cellulose beads. On the other hand, the untreated cellulose beads adsorbed only 0.035 g/g-cell of HA at pH 3. In addition, they adsorbed little HA at pH values higher than 6.

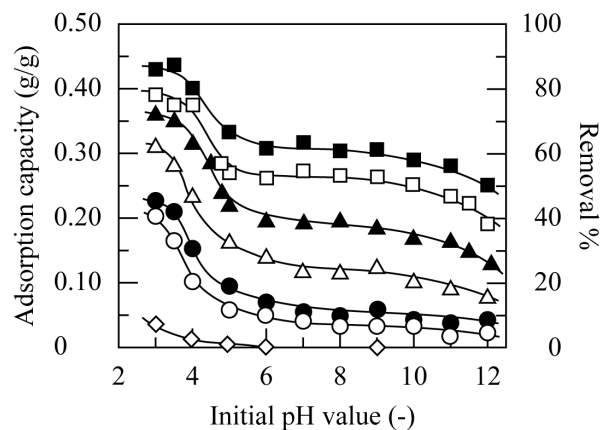


Figure 2. Changes in the adsorption capacity with the initial pH value for the untreated cellulose beads (◇) and the quaternized cellulose beads with 0.053 (○), 0.095 (●), 0.156 (△), 0.231 (▲), 0.380 (□), and 0.524 (■) mmol/g-Qcell in a 100 mg/L HA solution at 25 °C.

HA is a macromolecular compound [32,33], and the chemical properties are different depending on the source and extraction method. In common, an HA molecule carries multiple carboxy and phenolic hydroxy groups, although its structure varies with the geographical origin, age, climate, and biological conditions [6,34–36]. Here, since the number of carboxy groups is higher than that of phenolic hydroxy groups in an HA molecule and carboxy groups are more acidic than phenolic hydroxy groups, the pK_a value ranges from 4–6. Also, according to Shen et al., the pK_a value of Aldrich HA has been reported to be 4.26 [37]. The degree of dissociation of negatively chargeable functional groups was calculated to be 5 and 98% at pH 3 and 6, respectively, from the Henderson–Hasselbalch equation. Since adsorption of HA on the quaternized cellulose beads occurs mainly through the electrostatic interaction between a dissociated carboxy group affixed to an HA molecule and a quaternary ammonium group on the quaternized cellulose beads, the dissociation of carboxy groups affixed to the HA molecules remaining in the outer solution will be promoted due to the decrease in the concentration of dissociated carboxy groups through the adsorption.

In contrast, the increase in the pH value from 4 leads to the increase in the dissociation of negatively chargeable functional groups on the HA molecules. Accordingly, the radius of gyration, or hydrodynamic radius, of an HA molecule will increase by the intra-molecular electrostatic repulsion [38,39]. Also, the intermolecular electrostatic repulsion will occur between HA molecules binding to the quaternized cellulose beads and ones present in the outer solution. Such behavior will bring the reduction of HA adsorption. In addition, in the range of pH values higher than 4, the pH value at equilibrium was more or less different from the initial pH value, as reported in our previous article [21] (Figure S5). In the range of pH 4–7, the pH value a little increased by HA adsorption. This would be caused by the decrease in the HA concentration due to HA adsorption. At higher than pH 7, the pH value decreased by HA adsorption. In particular, the decrease in the pH value was remarkable in the range of pH 9–11. Such pH dependence by HA adsorption has been reported in other articles [40–44].

To sum up the above discussion, the decrease in the adsorption capacity can be explained in terms of the following concepts. Chlorine ions are released into the outer solution through the adsorption of HA on the quaternized cellulose beads, whereby the counter ion of a quaternary ammonium group is exchanged from a chloride anion to a hydroxy anion [45]. In addition, as the pH value of the HA solution increases, the hydrodynamic radius of an HA molecule increases due to the intermolecular electrostatic repulsion between negatively charged functional groups [46].

3.3.2. Effect of Temperature

The effect of the temperature on HA adsorption was estimated for the quaternized cellulose beads with 0.095, 0.231, and 0.380 mmol/g-Qcell at pH 3 and 6. Figure 3 shows the changes in the adsorption capacity, removal %, initial rate of adsorption, and $t_{1/2}$ value with the temperature. Here, $t_{1/2}$ is defined as the time taken for the adsorbed amount to reach half of its equilibrium value [47]. The adsorption capacity remained almost unchanged against the temperature, whereas the initial rate of adsorption increased and the $t_{1/2}$ value shortened with increased temperature. This indicates that adsorption behavior in this study depends on the temperature. Therefore, the kinetic analysis on the temperature dependence will be discussed in Section 3.4.2.

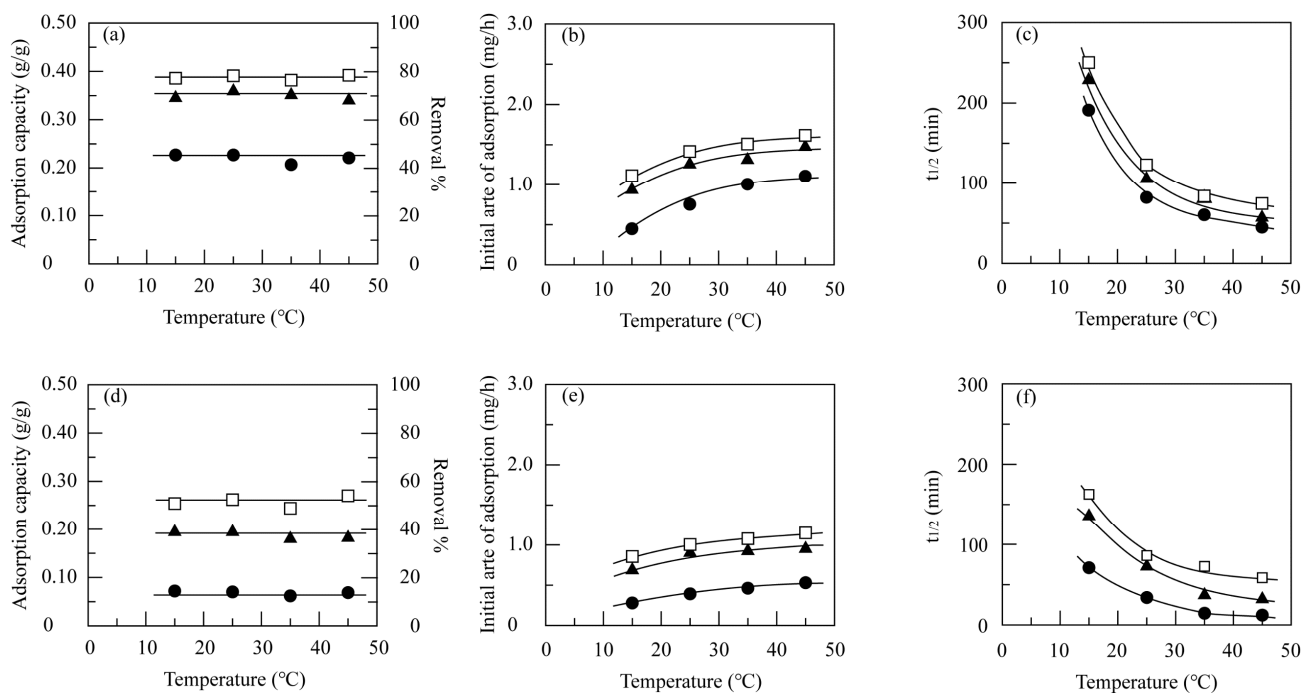


Figure 3. Changes in the adsorption capacity and removal % (a,d), initial rate of adsorption (b,e), and $t_{1/2}$ value (c,f) with the temperature at pH 3 (a–c) and 6 (d–f) for the quaternized cellulose beads at 0.095 (●), 0.231 (▲), and 0.380 (□) mmol/g-Qcell in a 100 mg/L HA solution at 25 °C.

3.3.3. Effect of the Dose of Quaternized Cellulose Beads

The dose of quaternized cellulose beads is also a factor to affect the HA adsorption. Figure 4 shows the changes in the net adsorbed amount, adsorption capacity, and removal % with the dose of quaternized cellulose beads for the quaternized cellulose beads with 0.231 mmol/g-Qcell at pH 3 and 6. The adsorption capacity was constant at lower than 20 mg and then gradually decreased at further increased doses at pH 6. On the other hand, at pH 3, the adsorption capacity sharply decreased with an increase in the dose of quaternized cellulose beads. The removal % higher than 95% was obtained in the range of the dose of quaternized cellulose beads of higher than 30 mg at pH 3 and of higher than 40 mg at pH 6, respectively.

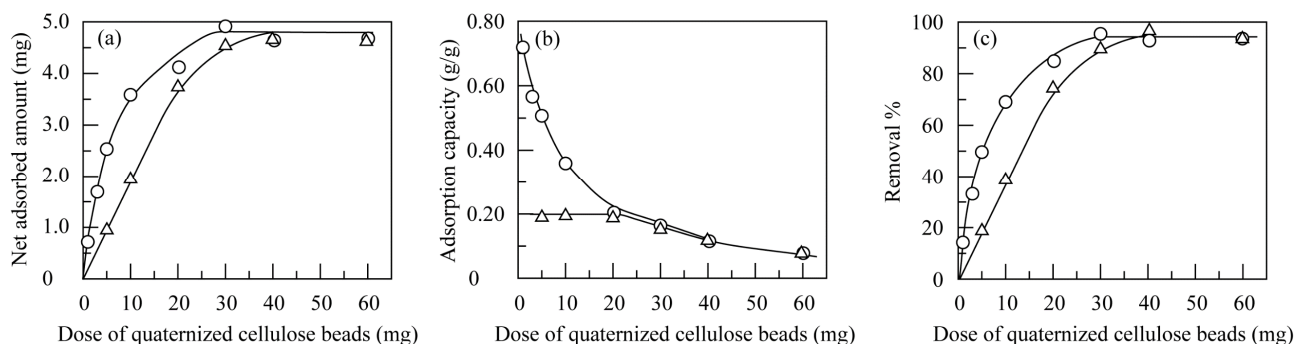


Figure 4. Changes in the (a) net adsorbed amount, (b) adsorption capacity, and (c) removal % with the dose of quaternized cellulose beads with 0.231 mmol/g-Qcell at pH 3 (○) and 6 (△).

Figure 5 shows the changes in the net adsorbed amount, adsorption capacity, and removal % with the dose of quaternized cellulose beads with different contents of quaternary ammonium groups at pH 6. The net adsorbed amount was directly proportional to the added dose and the adsorption capacity was constant at 0.053 mmol/g-Qcell. The range of the added dose in which the net adsorbed amount was directly proportional to the added dose and the adsorption capacity was constant became smaller at higher added doses. At pH 6, the removal % higher than 95% was obtained at 0.231 mmol/g-Qcell. In addition, as the content of quaternary ammonium groups increased, the added dose to obtain the removal % higher than 95% decreased. The adsorption capacity and removal % increased with an increase in the content of quaternary ammonium groups at both pH 3 and 6, as shown in Figure S6. These results indicate that HA can be effectively and highly removed from aqueous medium by using quaternized cellulose beads with higher quaternary ammonium groups.

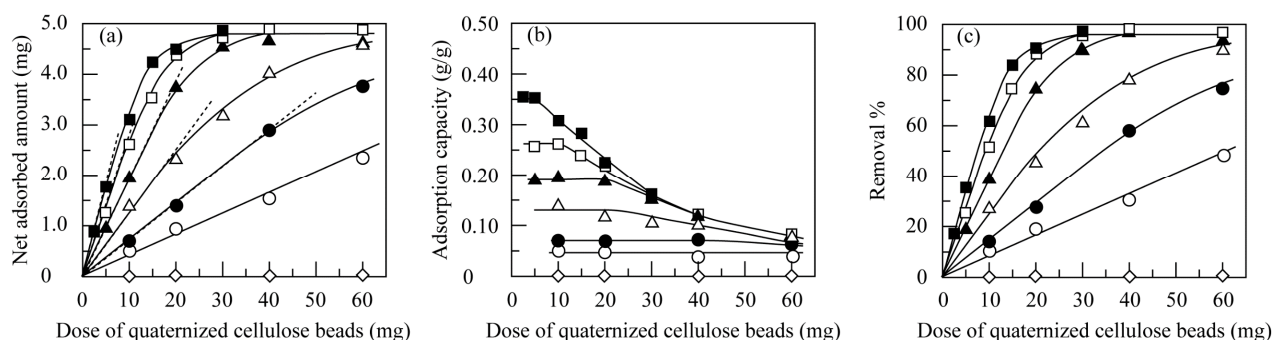


Figure 5. Changes in the (a) net adsorbed amount, (b) adsorption capacity, and (c) removal % with the dose of quaternized cellulose beads at 0.053 (○), 0.095 (●), 0.156 (△), 0.231 (▲), 0.380 (□), and 0.524 (■) mmol/g-Qcell and for the untreated cellulose beads (◇) in a 100 mg/L HA solution at pH 6.0.

3.4. Kinetic Analysis

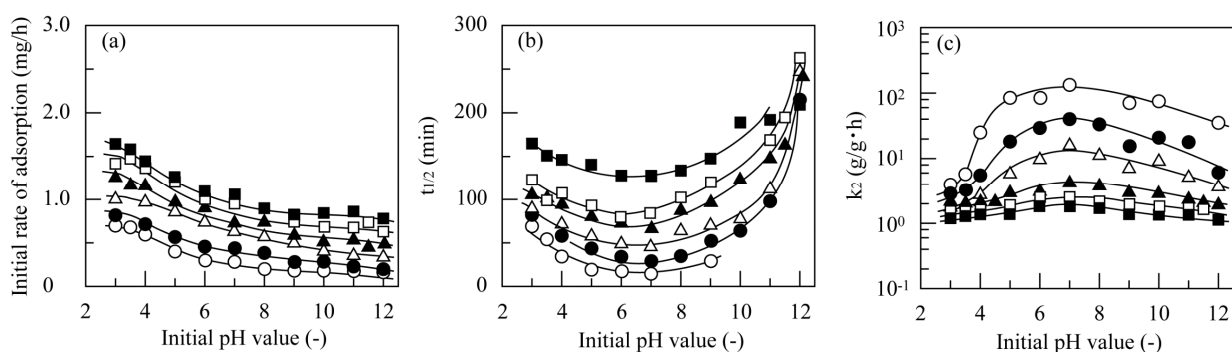
3.4.1. Effect of pH

The adsorption process at pH 3–12 for quaternized cellulose beads shown in Figure 2 was analyzed by the pseudo-first-order and pseudo-second-order models. The results were tabulated in Table 1 for the quaternized cellulose beads with 0.231 mmol/g-Qcell. The data were followed by the pseudo-first-order model within at least 10 min, or at most 40 min. Meanwhile, the data are well fit to the pseudo-second-order model for the immersion time of 5.5–7 h during which the adsorbed amount went up to 70–80% of the adsorption capacity with higher correlation coefficients. The values of adsorption capacity calculated by the pseudo-second-order equation were almost the same as the experimental values. These results indicate that the kinetics of HA adsorption in this study is followed by the pseudo-second-order equation. A high fit to the pseudo-second-order model suggests that the chemical interaction is responsible for HA adsorption.

Next, the effects of the pH value and temperature on HA adsorption will be discussed using the k_2 values obtained by the pseudo-second-order equation. Figure 6 shows the changes in the initial rate of adsorption, $t_{1/2}$ value, and k_2 value with the initial pH value for quaternized cellulose beads with different contents of quaternary ammonium groups. The adsorption capacity decreased with increasing pH value. On the other hand, the k_2 value increased with increasing pH value and reached the maximum at pH 6–7. In other words, a high k_2 value was obtained due to the fact that adsorption reached equilibrium at a short time.

Table 1. Kinetic parameters calculated pseudo-first-order and pseudo-second-order equations for adsorption of HA on the quaternized cellulose beads with 0.231 mmol/g-Qcell at pH 3–10.

pH	Q_{eq}^{exp} (g/g-Qcell)	Pseudo-First Order				Pseudo-Second Order			
		Q_{eq}^{cal} (g/g-Qcell)	k_1 (1/h)	R^2	Range (min)	Q_{eq}^{cal} (g/g-Qcell)	k_2 (g/g·h)	r^2	Range (h)
3.0	0.359	0.350	1.67	0.9088	5	0.358	2.17	0.9961	6.58
4.0	0.314	0.299	0.55	0.9973	30	0.318	2.12	0.9970	6.75
5.0	0.218	0.211	1.38	0.9675	20	0.220	2.94	0.9993	5.67
6.0	0.194	0.191	0.50	0.9952	40	0.193	3.08	0.9996	5.93
7.0	0.191	0.199	0.47	0.9817	30	0.197	2.83	0.9975	6.50
8.0	0.194	0.188	0.63	0.9733	25	0.191	3.76	0.9996	4.83
9.0	0.183	0.190	1.23	0.9938	5	0.180	2.96	0.9976	6.33
10.0	0.167	0.178	0.44	0.9786	40	0.175	2.86	0.9917	6.75
11.0	0.166	0.160	0.50	0.9635	30	0.169	2.83	0.9991	6.33
12.0	0.128	0.137	0.44	0.9489	30	0.148	1.91	0.9952	5.67

**Figure 6.** Changes in the (a) initial rate of adsorption, (b) $t_{1/2}$, and (c) k_2 with the initial pH value for the quaternized cellulose beads with 0.053 (○), 0.095 (●), 0.156 (△), 0.231 (▲), 0.380 (□), and 0.524 (■) mmol/g-Qcell in a 100 mg/L HA solution.

However, as the initial pH value increased, the initial rate as well as the adsorption capacity decreased due to the fact that the dissociation of carboxy groups on an HA molecule are facilitated [48]. For these reasons, the k_2 value will gradually decrease with an increase in the pH value. In addition, the initial rate and $t_{1/2}$ value were higher and it took longer time to reach the adsorption equilibrium at higher content of quaternary ammonium groups. Therefore, the higher the content of quaternary ammonium groups, the lower the k_2 value. The diffusivity of HA molecules, which decreases with increasing pH value, would be also involved in HA adsorption [49].

3.4.2. Effect of Temperature

The results of pseudo-second-order analysis are shown in Table 2 for HA adsorption on the quaternized cellulose beads with 0.231 mmol/g-Qcell in the temperature range from 15 to 45 °C at pH 3 and 6. The calculated values agreed well with the values of adsorption capacity and the increase in the temperature led to the increase in the k_2 value. In addition, the activation energy, E , was calculated from the Arrhenius equation shown in Equation (10).

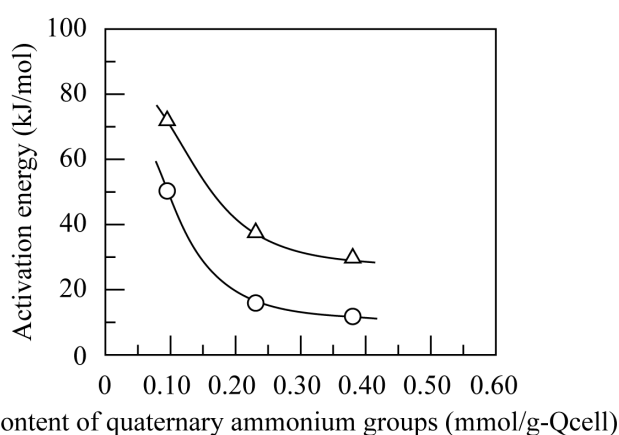
$$\ln k_2 = -\frac{E}{RT} + \ln A \quad (10)$$

where A is a term that includes factors like the frequency of collisions (g/mol·s) and R is the universal gas constant (8.314 J/K·mol) [50–52].

Table 2. Kinetic parameters calculated by the pseudo-second-order equation for adsorption of HA on the quaternized cellulose beads with 0.231 mmol/g-Qcell at 15–45 °C.

at pH 3.0					
Temp.	Q_{eq}^{exp}	Q_{eq}^{cal}	k_2	r^2	Range
(°C)	(g/g-Qcell)	(g/g-Qcell)	(g/g·h)		(h)
15	0.345	0.338	1.46	0.9872	5.50
25	0.359	0.358	2.17	0.9961	6.58
35	0.344	0.342	2.29	0.9991	6.58
45	0.340	0.336	2.59	0.9962	6.08
at pH 6.0					
Temp.	Q_{eq}^{exp}	Q_{eq}^{cal}	k_2	r^2	Range
(°C)	(g/g-Qcell)	(g/g-Qcell)	(g/g·h)		(h)
15	0.194	0.194	2.01	0.9969	6.67
25	0.194	0.193	3.08	0.9996	5.93
35	0.180	0.181	5.88	0.9994	6.83
45	0.182	0.179	8.77	0.9932	6.98

Since a good linear relationship held between $1/T$ and $\ln k_2$, the activation energy was calculated from the slope. As shown in Figure 7, the activation energy decreased with an increase in the content of quaternary ammonium groups, and their values were much higher than 4.2 kJ/mol. If an adsorbate molecule is held on the adsorbent surface mainly by van der Waals type of interaction, the activation energy is usually no more than 4.2 kJ/mol [50–52]. Therefore, the results shown in Figure 7 indicate that HA adsorption on the quaternized cellulose beads is controlled by chemical reaction. In short, this synthesizes that HA adsorption will occur by the electrostatic interaction of a dissociated carboxy group on an HA molecule with a quaternary ammonium group on the quaternized cellulose beads through the ion exchange interaction. In addition, these results suggest that HA adsorption is facilitated by a lower energy barrier at pH 3 and/or at higher contents of quaternary ammonium groups. This supports that higher adsorption capacity was obtained at lower pH values and/or at higher contents of quaternary ammonium groups. In particular, the decrease in the activation energy shown in Figure 7 can result from the hydrophilization of the surfaces of the cellulose beads by introducing quaternary ammonium groups.

**Figure 7.** Changes in the activation energy with the content of quaternary ammonium groups at pH 3.0 (○) and 6.0 (△).

3.4.3. Effect of Dose of Quantized Cellulose Beads

The changes in the k_2 value as well as the initial rate and $t_{1/2}$ value with the dose of quaternized cellulose beads are shown in Figure 8. At 0.053 mmol/g-Qcell, both removal % and initial rate were directly proportional to the dose of quaternized cellulose beads, and $t_{1/2}$ and k_2 values were constant against the dose of quaternized cellulose beads. As the content of quaternary ammonium groups further increased, the initial rate became higher, whereas the $t_{1/2}$ value also increased. Such a result is explained in terms of the fact that it takes longer time to attain the equilibrium at higher contents of quaternary ammonium groups. The initial rate increased in the case where the dose of quaternized cellulose beads was increased. At removal % higher than 80%, the $t_{1/2}$ and k_2 values could not be determined due to shortage of HA in the solution.

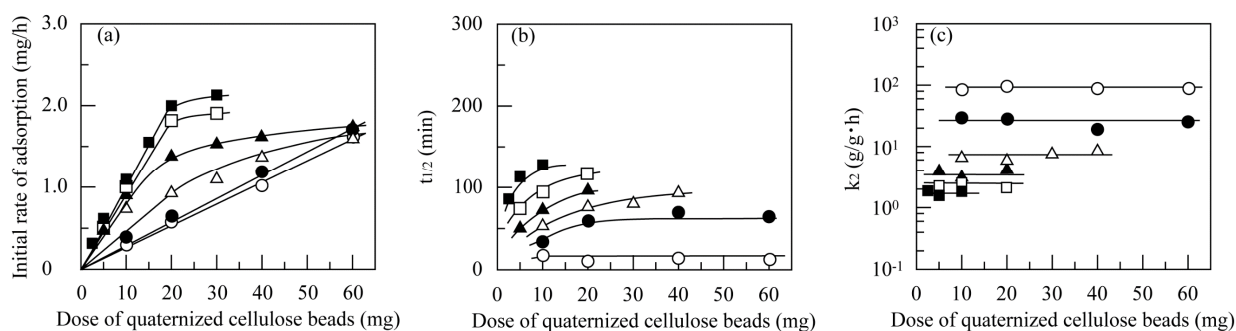


Figure 8. Changes in the (a) initial rate of adsorption, (b) $t_{1/2}$, and (c) k_2 with the dose of quaternized cellulose beads at 0.053 (○), 0.095 (●), 0.156 (△), 0.231 (▲), 0.380 (□), and 0.524 (■) mmol/g-Qcell in a 100 mg/L HA solution at pH 6.0.

To summarize the above results, the k_2 value depends on the initial pH, temperature, and content of quaternary ammonium groups, whereas little depends on the dose of quaternized cellulose beads [53–55]. Many articles on the effects of the above experimental factors on the k_2 value have been published, and little has been reported on the k_2 value in terms of the content of quaternary ammonium groups. Therefore, some novel findings can be shown on the kinetics for HA adsorption in this study.

3.5. Isotherm Analysis

The adsorption capacity was obtained at different HA concentrations for quaternized cellulose beads with 0.095, 0.231, and 0.380 mmol/g-Qcell at pH 3 and 6, and the equilibrium data were analyzed using Langmuir and Freundlich isotherm equations. Under the above conditions, the adsorption capacity increased and removal % decreased with increasing initial HA concentration.

The Langmuir and Freundlich isotherms in their linear forms are shown in Figure S7. The Langmuir isotherm provided a linear relationship with a high correlation coefficient for the quaternized cellulose beads with 0.231 mmol/g-Qcell. Therefore, the results obtained from Langmuir isotherm are summarized in Table 3 along with the other two quaternized cellulose beads. The adsorption processes followed the Langmuir isotherm with higher correlation coefficients. Higher Langmuir constants were obtained at pH 3 and/or at higher contents of quaternary ammonium groups. These results firmly support the fact that HA adsorption more successfully proceeds at lower pH values and/or at higher contents of quaternary ammonium groups. This means that the adsorption process is achieved through a stoichiometric reaction, or through the mechanism described in Section 3.4.2. Here, the maximum value of the Q_{max} value of 0.861 g/g was obtained at pH 3 for the quaternized cellulose beads with 0.380 mmol/g-Qcell. The comparison of this value with those in other articles will be discussed in Section 3.7.

Table 3. The Langmuir and Freundlich parameters for adsorption of HA on the quaternized cellulose beads with 0.095, 0.231, and 0.380 mmol/g-Qcell at pH 3.0 and 6.0.

$A_{\text{quater}}^{\text{Qcell}}$ (mmol/g-Qcell)	pH	C_0 (mg/L)	Q_{max} (g/g-Qcell)	K_L (L/mg)	r^2	R_L (-)
0.095	3.0	55.2–148.8	0.431	0.0196	0.9877	0.255–0.480
	6.0	50.8–146.6	0.119	0.0188	0.9916	0.266–0.512
0.231	3.0	65.4–153.3	0.770	0.0279	0.9851	0.189–0.354
	6.0	77.8–149.8	0.354	0.0196	0.9970	0.254–0.396
0.380	3.0	82.7–175.9	0.861	0.0308	0.9977	0.156–0.282
	6.0	80.3–177.6	0.487	0.0151	0.9937	0.184–0.332

In addition, the essential characteristic of Langmuir equation was discussed using the dimensionless separation factor, R_L , defined by Equation (11) [56–58].

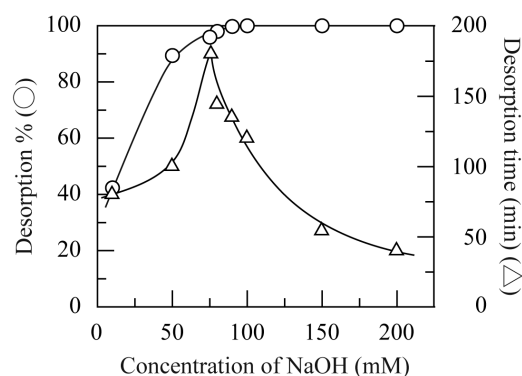
$$R_L = \frac{1}{1 + K_L \cdot C_0} \quad (11)$$

Here, there are four possible outcomes of the R_L value for the type of Langmuir isotherm, such as irreversible ($R_L = 0$), favorable ($0 < R_L < 1$), linear ($R_L = 1$), or unfavorable ($R_L > 1$).

In this study, the R_L values lay between 0 and 1, as shown in Table 3. In addition, the R_L value decreased as the pH value decreased and/or the content of quaternary ammonium groups decreased. These results suggest that the HA adsorption process is favorable and the quaternized cellulose beads can be regenerated and applied to the successive adsorption–desorption cycles.

3.6. Desorption of HA

The quaternized cellulose beads with 0.231 mmol/g-Qcell loaded with HA at pH 6 were immersed in NaOH solutions for desorption of HA [59]. The changes in the desorption % and desorption time with the NaOH concentration are shown in Figure 9. Here, the adsorbed amount of 0.155 g/g obtained by immersion for 15–16 h was almost constant (0.143–0.166 g/g). Higher desorption % values were obtained at higher NaOH concentrations and HA was completely released at higher than 100 mM. In addition, the desorption time was shortened with increasing NaOH concentration in the range of concentrations higher than 75 mM. Next, five cycles of adsorption at pH 6 and desorption in a 100 mM NaOH solution were successively performed. As shown in Figure 10, even when the adsorption and desorption cycle was repeated five times, desorption % was almost constant and desorption of HA successfully occurred in each cycle. It was found from this result that the quaternized cellulose beads were regenerated without considerable reduction in the adsorption capacity.

**Figure 9.** Changes in the desorption % and desorption time with the concentration of NaOH for the quaternized cellulose beads with 0.231 mmol/g-Qcell at 25 °C.

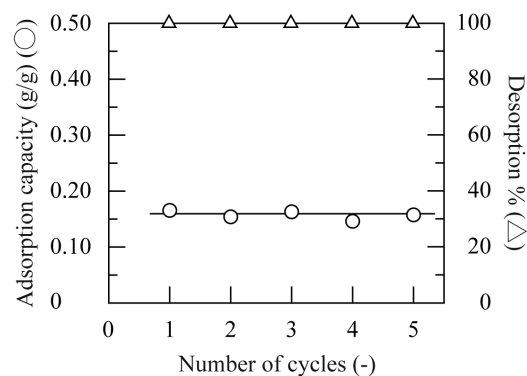


Figure 10. The repetitive cycles of adsorption in a 100 mg/L HA solution at pH 6.0 and desorption in a 100 mM NaOH solution for the quaternized cellulose beads with 0.231 mmol/g-Qcell at 25 °C.

3.7. Comparison with Other Adsorbents

The adsorption capacity was 430 and 312 mg/g-Qcell, respectively, for the quaternized cellulose beads with 0.524 mmol/g-Qcell. The adsorption capacity of 575 mg/g was obtained at 175 mg/L and pH 3 for the quaternized cellulose beads with 0.380 mmol/g. These values were compared with ones published in other articles [6,14,40,43,44,48,60–62]. Here, one should bear in mind that the experimental parameters, such as the initial pH value, temperature, HA concentration, volume of HA solution, and dose of adsorbent, vary from article to article. The values of adsorption capacity obtained in other articles are summarized in Table 4 along with the important experimental conditions. Although it is difficult to compare our adsorption capacity with others, the adsorption capacity obtained in this study was far higher than many of the other adsorbents in spite of the fact that our HA concentration was lower than those in others. From these results, we can emphasize that the quaternized cellulose beads with a high adsorption capacity toward HA were prepared and they have a high potentiality as adsorbent for removal of HA from aqueous medium.

Table 4. The comparison with HA adsorption capacities of adsorbents reported in other articles.

Adsorbent	pH	Temp. (°C)	HA Conc. (mg/L)	Dose (g/L)	Qexp (mg/g)	Qmax (mg/g)	Ref.
Quaternized cellulose beads	3.0	25	100	0.20	430		this study
with 0.524 mmol/g-Qcell	6.0	25	100	0.20	312		
Quaternized cellulose beads	3.0	25	175	0.20	575	861	
with 0.524 mmol/g-Qcell	6.0	25	100	0.20	365	487	
Zeolite-coated zero-valent iron particles	3	25	100	0.10	42.1	36.23	[6]
Activated carbon from rice husks	6.5	25	10	1.0	27.4	30.4	[14]
Aminated polyacrylonitrile fibers	6	22–23	50	2.0	9.7	16.22	[40]
Surfactant-modified chitosan/zeolite	7	30	90	0.50	164		[43]
PDMAEMA/pumice composite hydrogel	4.0	20	50	0.50	59.72		[44]
Al ³⁺ -based metal organic framework	natural	30	25	0.50	33.67	115.5	[48]
PEI modified magnetic graphite	6.5	20	21	0.25	39.76	50.68	[60]
Amine-modified silica aerogel	5.0	5	250	1	235.5		[61]
Cobalt-based metal-organic framework	6	32	50	0.50	89.72		[62]

4. Conclusions

In this study, the quaternized cellulose beads with different content of quaternary ammonium groups were prepared and their HA adsorption behavior was investigated by varying the experimental conditions. In addition, the kinetic, isothermal, and thermodynamic studies were also performed for their application as a promising adsorbent. Since the FT-IR and XPS analysis showed the presence of quaternary ammonium groups on the cellulose beads, the content of quaternary ammonium groups was determined by back titration. The content of quaternary ammonium groups increased to 0.524 mmol/g-Qcell

corresponding to 0.569 mmol/g-cell by increasing the GTMAC concentration. The adsorption capacity increased with a decrease in the pH value and the maximum adsorption capacity was obtained at pH 3.0. On the other hand, the increase in the temperature led to the k_2 value obtained from the pseudo-second-order equation, while the adsorption capacity remained unchanged. The kinetics of HA adsorption obeyed the pseudo-second-order model and the adsorption capacity was well described by the Langmuir isotherm. These results emphasize that the HA adsorption will occur through the chemical bonding (interaction), or the electrostatic interaction between a dissociated carboxy group of an HA molecule and a quaternary ammonium group on the quaternized cellulose beads. The removal % value increased with the increase in the content of quaternary ammonium groups and/or the dose of quaternized cellulose beads. The removal % values over 90% were obtained by adding the quaternized cellulose beads with higher than 0.380 mmol/g-Qcell, indicating that HA was almost completely removed from the aqueous medium. The adsorption capacity obtained in this study was higher than those of other articles. In addition, the quaternized cellulose beads were repeatedly used without appreciable loss in the adsorption capacity. Finally, our study provides a new prospective on the sustainable purification of HA-containing waters with the quaternized cellulose beads and extends their application in environmental remediation. Therefore, our next target is to design and operate the fixed-bed adsorption systems for HA removal.

Supplementary Materials: The following supporting information can be downloaded at: <https://www.mdpi.com/article/10.3390/macromol4010006/s1>, Figure S1: The FT-IR spectra of (a) the untreated cellulose beads and (b) the quaternized cellulose beads with 0.524 mmol/g; Figure S2: The XPS high-resolution spectra of C_{1s} , O_{1s} , N_{1s} , and Cl_{2p} for (a) the untreated cellulose beads and the quaternized cellulose beads with 0.231 mmol/g (b) before and (c) after treatment with NaOH; Figure S3: Change in the water content with the content of quaternary ammonium groups at 25 °C; Figure S4: The particle distributions for the quaternized cellulose beads with 0.231 mmol/g-Qcell in the (a) dry and (b) water-swollen state at 25 °C; Table S1. The particle sizes of the untreated and quaternized cellulose beads with different contents of quaternary ammonium groups in the dry and water-swollen states; Figure S5 Changes in the pH value for adsorption on the quaternized cellulose beads with 0.053 (○), 0.095 (●), 0.156 (△), 0.231 (▲), 0.380 (□), and 0.524 (■) mmol/g-Qcell in a 100 mg/L HA solution at 25 °C; Figure S6 Changes in the adsorption capacity and removal % with the content of quaternary ammonium groups in a 100 mg/L HA solution at pH 3.0 (○) and 6.0 (△); Figure S7 Determination of (a) the pseudo-first-order constant, k_1 , and (b) pseudo-second-order constant, k_2 , for adsorption of HA on the quaternized cellulose beads with 0.231 mmol/g-Qcell in a 100 mg/L HA solution at pH 3.0 and 30 °C.

Author Contributions: Conceptualization, H.M. and K.Y.; methodology, H.A., H.M. and K.Y.; validation, H.A. and K.Y.; investigation, K.U.; resources, K.Y.; data curation, K.U. and K.Y.; writing—original draft preparation, K.Y.; writing—review and editing, H.A., H.M. and K.Y.; visualization, K.U. and K.Y.; supervision, K.Y.; project administration, K.Y. All authors have read and agreed to the published version of the manuscript.

Funding: This research received no external funding.

Institutional Review Board Statement: Not applicable.

Informed Consent Statement: Not applicable.

Data Availability Statement: All the data are available within the manuscript.

Conflicts of Interest: The authors declare no conflicts of interest.

References

1. Klučáková, M.; Pelikán, P.; Lapčík, L.; Lapčíková, B.; Kučerík, J.; Kaláb, M. Structure and properties of humic and fulvic acids. 1. Properties and reactivity of humic acids and fulvic acids. *J. Polym. Mater.* **2000**, *17*, 337–356.
2. Jarukas, L.; Ivanauskas, L.; Kasparaviciene, G.; Baranauskaitė, J.; Marksa, M.; Bernatoniene, J. Determination of organic compounds, fulvic acid, humic acid, and humin in peat and sapropel alkaline extracts. *Molecules* **2021**, *26*, 2995. [[CrossRef](#)]

3. Mirza, M.A.; Agarwal, S.P.; Rahman, M.K.; Rauf, A.; Ahmad, N.; Alam, A.; Iqbal, Z. Role of humic acid on oral drug delivery of an antiepileptic drug. *Drug Dev. Ind. Pharm.* **2011**, *37*, 310–319. [[CrossRef](#)]
4. Rupiasih, N.N.; Vidyasagar, P.B. A review: Compositions, structures, properties and applications of humic substances. *J. Adv. Sci. Technol.* **2005**, *8*, 16–25.
5. Noroozisharaf, A.; Kaviani, M. Effect of soil application of humic acid on nutrients uptake, essential oil and chemical compositions of garden thyme (*Thymus vulgaris* L.) under greenhouse conditions. *Physiol. Mol. Biol. Plants* **2018**, *24*, 423–431. [[CrossRef](#)] [[PubMed](#)]
6. Almar, T.; Qiblaway, H.; Almomani, F.; Al-Raoush, R.; Han, D.S.; Ahmad, N.M. Recent advances on humic acid removal from wastewater using adsorption process. *J. Water Process Eng.* **2023**, *53*, 103679. [[CrossRef](#)]
7. García-Mina, J.M.; Antolín, M.C.; Sanchez-Diaz, M. Metal-humic complexes and plant micronutrient uptake: A study based on different plant species cultivated in diverse soil types. *Plant Soil* **2004**, *258*, 57–58. [[CrossRef](#)]
8. Nikolaou, A.D.; Goulinopoulos, S.K.; Lekkas, T.D.; Kostopoulou, M.N. DBP levels in chlorinated drinking water: Effect of humic substances. *Environ. Monit. Assess.* **2004**, *93*, 301–319. [[CrossRef](#)]
9. Deborde, M.; von Gunten, U. Reactions of chlorine with inorganic and organic compounds during water treatment-Kinetics and mechanisms: A critical review. *Water Res.* **2008**, *42*, 13–51. [[CrossRef](#)]
10. Hakim, A.; Suzuki, T.; Kobayashi, M. Strength of Humic Acid Aggregates: Effects of Divalent Cations and Solution pH. *ACS Omega* **2019**, *4*, 8559–8567. [[CrossRef](#)]
11. Zhu, X.; Liu, J.; Li, L.; Zhen, G.; Lu, X.; Zhang, J.; Liu, H.; Zhou, Z.; Wu, Z.; Zhang, X. Prospects for humic acids treatment and recovery in wastewater: A review. *Chemosphere* **2023**, *312*, 137193. [[CrossRef](#)] [[PubMed](#)]
12. Grace, M.A.; Clifford, E.; Healy, M.G. The potential for the use of waste products from a variety of sectors in water treatment processes. *J. Clean. Prod.* **2016**, *137*, 788–802. [[CrossRef](#)]
13. Duran, C.; Ozdes, D.; Gundogdu, A.; Senturk, H.B. Kinetics and isotherm analysis of basic dyes adsorption onto almond shell (*Prunus dulcis*) as a low cost adsorbent. *J. Chem. Eng. Data* **2011**, *56*, 2136–2147. [[CrossRef](#)]
14. Menya, E.; Olupot, P.W.; Storz, H.; Lubwama, M.; Kiros, Y. Synthesis and evaluation of activated carbon from rice husks for removal of humic acid from water. *Biomass Conv. Bioref.* **2022**, *26*, 3229–3248. [[CrossRef](#)]
15. Kołodziej, A.; Fuentes, M.; Baigorri, R.; Lorenc-Brabowska, E.; García-Mina, J.M.; Burg, P.; Gryglewicz, G. Mechanism of adsorption of different humic acid fractions on mesoporous activated carbons with basic surface characteristics. *Adsorption* **2014**, *20*, 667–675. [[CrossRef](#)]
16. Eustáquio, H.M.B.; Lopes, C.W.; da Rocha, R.S.; Cardoso, B.D.; Pergher, S.B.C. Modification of activated carbon for the adsorption of humic acid. *Adsorpt. Sci. Technol.* **2015**, *33*, 117–126. [[CrossRef](#)]
17. Habuta-stanić, M.; Tutić, A.; Grgić, D.K.; Zeko-Pivač, A.; Burilo, A.; Paixão, S.; Teixeira, V.; Pagaimo, M.; Pala, A.; Ravančić, M.E.; et al. Adsorption of humic acid from water using chemically modified bituminous coal-based activated carbons. *Chem. Biochem. Eng. Q.* **2021**, *35*, 189–203. [[CrossRef](#)]
18. Hishikawa, Y.; Togawa, E.; Kondo, T. Characterization of individual hydrogen bonds in crystalline regenerated cellulose using resolved polarized FTIR spectra. *ACS Omega* **2017**, *2*, 1469–1476. [[CrossRef](#)]
19. Hokkanen, S.; Bhatnagar, A.; Sillanpää, M. A review on modification methods to cellulose-based adsorbents to improve adsorption capacity. *Water Res.* **2016**, *91*, 156–173. [[CrossRef](#)]
20. Suhas; Gupta, V.K.; Carrott, P.J.M.; Singh, R.; Chaudhary, M.; Kushwaha, S. Cellulose: A review as natural, modified and activated carbon adsorbent. *Bioresour. Technol.* **2016**, *216*, 1066–1076. [[CrossRef](#)] [[PubMed](#)]
21. Uchiyama, K.; Asamoto, H.; Minamisawa, H.; Yamada, K. Quaternization of porous cellulose beads and their use for removal of humic acid from aqueous medium. *Physchem* **2023**, *3*, 61–76. [[CrossRef](#)]
22. Sehaqui, H.; de Larraya, U.P.; Tingaut, P.; Zimmermann, T. Humic acid adsorption onto cationic cellulose nanofibers for bioinspired removal of copper(II) and a positively charged dye. *Soft Matter* **2015**, *11*, 5294–5300. [[CrossRef](#)]
23. Revellame, E.D.; Fortela, D.L.; Sharp, W.; Hernandez, R.; Zappi, M.E. Adsorption kinetic modeling using pseudo-first order and pseudo-second order rate laws: A review. *Clean. Eng. Technol.* **2020**, *1*, 100032. [[CrossRef](#)]
24. Tan, K.L.; Hameed, B.H. Insight into the adsorption kinetics models for the removal of contaminants from aqueous solutions. *J. Taiwan Inst. Chem. Eng.* **2017**, *74*, 25–48. [[CrossRef](#)]
25. Langmuir, I. The adsorption of gases on plane surfaces of glass, mica and platinum. *J. Am. Chem. Soc.* **1918**, *40*, 1361–1403. [[CrossRef](#)]
26. Freundlich, H. Über die Adsorption in Lösungen. *Z. Phys. Chem.* **1907**, *57*, 385–470. [[CrossRef](#)]
27. Debord, J.; Chu, K.H.; Salvestrini, S.; Bollinger, J. Yesterday, today, and tomorrow. Evolution of a sleeping beauty: The Freundlich isotherm. *Langmuir* **2023**, *39*, 3062–3071. [[CrossRef](#)]
28. Song, Y.; Zhang, L.; Gan, W.; Zhou, J.; Zhang, L. Self-assembled based on hydrophobically modified quaternized cellulose for drug delivery. *Colloids Surf. B Biointerfaces* **2011**, *83*, 313–320. [[CrossRef](#)]
29. Roshan, K.R.; Jose, T.; Kathalikkatti, A.C.; Kim, D.W.; Kim, B.; Park, D.W. Microwave synthesized quaternized cellulose for cyclic carbonate synthesis from carbon dioxide and epoxides. *Appl. Catal. A Gen.* **2013**, *467*, 17–25. [[CrossRef](#)]
30. Du, J.; Dong, Z.; Pi, Y.; Yang, X.; Zhao, L. Fabrication of cotton linter-based adsorbents by radiation grafting polymerization for humic acid removal from aqueous solution. *Polymers* **2019**, *11*, 962. [[CrossRef](#)]

31. Zhang, R.; Leiviskä, T. Surface modification of pine bark with quaternary ammonium groups and its use for vanadium removal. *Chem. Eng. J.* **2020**, *385*, 123967. [[CrossRef](#)]
32. de Mero, B.A.G.; Motta, F.L.; Santana, M.H.A. Humic acids: Structural properties and multiple functionalities for novel technological developments. *Mater. Sci. Eng.* **2016**, *C62*, 967–974. [[CrossRef](#)]
33. Capasso, S.; Chianese, S.; Musmarra, D.; Iovino, P. Macromolecular structure of a commercial humic acid sample. *Environments* **2020**, *7*, 32. [[CrossRef](#)]
34. de Aguiar, T.C.; Torchia, D.F.D.; de Castro, T.V.A.; Tavares, O.C.H.; Lopes, S.D.; da Silva, L.D.; Castro, R.N.; Berbara, R.L.L.; Pereira, M.G.; Garcia, A.C. Spectroscopic-chemometric modeling of 80 humic acids confirms the structural pattern identity of humified organic matter despite different formation environments. *Sci. Total Environ.* **2022**, *833*, 155133. [[CrossRef](#)]
35. Zhao, H.; Zhou, F.; Bao, X.; Zhou, S.; Wei, Z.; Long, W.; Yi, Z. A review on the humic substances in pelletizing binders: Preparation, interaction mechanism, and process characteristics. *ISIJ Int.* **2023**, *63*, 205–215. [[CrossRef](#)]
36. Ahmed, Z.; Yusoff, M.S.; Kamal, N.H.M.; Aziz, H.A.; Roulia, M. Spectroscopic and microscopic analysis of humic acid isolated from stabilized leachate HSs fractionation. *Agronomy* **2023**, *13*, 1160. [[CrossRef](#)]
37. Shen, J.; Yang, X.; Schäfer, A.I. Quantification of hormone-humic acid interactions in nanofiltration. *Environ. Sci. Technol.* **2012**, *46*, 10597–10604. [[CrossRef](#)] [[PubMed](#)]
38. Klučáková, M.; Kolajová, R. Dissociation ability of humic acids: Spectroscopic determination of pK_a and comparison with multi-step mechanism. *React. Funct. Polym.* **2014**, *78*, 1–6. [[CrossRef](#)]
39. Wang, Y.; Combe, C.; Clark, M.M. The effects of pH and calcium on the diffusion coefficient of humic acid. *J. Membr. Sci.* **2001**, *183*, 49–60. [[CrossRef](#)]
40. Deng, S.; Bai, R. Adsorption and desorption of humic acid on aminated polyacrylonitrile fibers. *J. Colloid Interface Sci.* **2004**, *280*, 36–43. [[CrossRef](#)] [[PubMed](#)]
41. Deng, S.; Yu, G.; Ting, Y.P. Removal of humic acid using PEI-modified fungal biomass. *Sep. Sci. Technol.* **2006**, *41*, 2989–3002. [[CrossRef](#)]
42. Illés, E.; Tombácz, E. The effect of humic adsorption on pH-dependent surface charging and aggregation of magnetite nanoparticles. *J. Colloid Interface Sci.* **2006**, *295*, 115–123. [[CrossRef](#)]
43. Lin, J.; Zhan, Y. Adsorption of humic acid from aqueous solution onto unmodified and surfactant-modified chitosan/zeolite composites. *Chem. Eng. J.* **2012**, *200–202*, 202–213. [[CrossRef](#)]
44. Taktak, F.; İlbaý, Z. Synthesis of novel poly[2-(dimethylamino) ethyl methacrylate]/pumice stone hydrogel composite for the rapid adsorption of humic acid in aqueous solution. *J. Macromol. Sci. A Pure Appl. Chem.* **2015**, *52*, 307–315. [[CrossRef](#)]
45. Rashtbari, Y.; Américo-Pinheiro, J.H.P.; Bahrami, S.; Fazlzadeh, M.; Arfaeina, H.; Poureshgh, Y. Efficiency of zeolite coated with zero-valent ion nanoparticles for removal of humic acid from aqueous solutions. *Water Air Soil Pollut.* **2020**, *231*, 514. [[CrossRef](#)]
46. Klučáková, M. Size and charge evaluation of standard humic and fulvic acids as crucial factors to determine their environmental behavior and impact. *Front. Chem.* **2018**, *6*, 235. [[CrossRef](#)] [[PubMed](#)]
47. Hubbe, M.A.; Azizian, S.; Douven, S. Implications of apparent pseudo-second-order adsorption kinetics onto cellulose materials: A review. *Bioresources* **2019**, *14*, 7582–7626. [[CrossRef](#)]
48. Zhao, X.; Wang, T.; Du, G.; Zheng, M.; Liu, S.; Zhang, Z.; Zhang, Y.; Gao, X.; Gao, Z.J. Effective removal of humic acid from aqueous solution in an Al-based metal–organic framework. *Chem. Eng. Data* **2019**, *64*, 3624–3631. [[CrossRef](#)]
49. Petrov, D.; Tunega, D.; Gerzabek, M.H.; Oostenbrink, C. Molecular dynamics simulations of the standard leonardite humic acid: Microscopic analysis of the structure and dynamics. *Environ. Sci. Technol.* **2017**, *51*, 5414–5424. [[CrossRef](#)] [[PubMed](#)]
50. Ahmad, R.; Haseeb, S. Adsorption of Pb(II) on *Mentha piperita* carbon (MTC) in single and quaternary systems. *Arab. J. Chem.* **2014**, *10*, S412–S421. [[CrossRef](#)]
51. Onursal, N.; Altunkaynak, Y.; Baran, A.; Del, M.C. Adsorption of nickel(II) ions from aqueous solutions using Malatya clay: Equilibrium, kinetic and thermodynamic studies. *Environ. Prog. Sustain. Energy* **2023**, *42*, e14150. [[CrossRef](#)]
52. Jankovic, J.; Lukic, J.; Kolarski, D.; Veljović, D.; Radovanović, Ž.; Dimitrijević, S. Isotherm, thermodynamic and kinetic studies of elemental sulfur removal from mineral insulating oils using highly selective adsorbent. *Materials* **2023**, *16*, 3522. [[CrossRef](#)] [[PubMed](#)]
53. Foo, K.Y.; Hameed, B.H. Insights into the modeling of adsorption isotherm systems. *Chem. Eng. J.* **2010**, *156*, 2–10. [[CrossRef](#)]
54. Webber, T.W.; Chakkaravorti, R.K. Pore and solid diffusion models for fixed-bed adsorbers. *AIChE J.* **1974**, *20*, 228–238. [[CrossRef](#)]
55. Akpromie, K.G.; Conradie, J.; Adegoke, K.A.; Oyedotun, K.O.; Ighalo, J.O.; Amaku, J.F.; Olisah, C.; Adeola, A.O.; Iwuozor, K.O. Adsorption mechanism and modeling of radionuclides and heavy metals onto ZnO nanoparticles: A review. *Appl. Water Sci.* **2023**, *13*, 20. [[CrossRef](#)]
56. Cumming, J.; Hawker, D.W.; Chapman, H.; Nugent, K. Sorption of polymeric quaternary ammonium compounds to humic acid. *Water Air Pollut.* **2011**, *214*, 5–11. [[CrossRef](#)]
57. Roba, C.A.; Jimenez, C.; Baciú, C.; Beldean-Galea, S.; Levei, E.; Cordoş, E. Assessment of different sorbents efficiency for solid phase extraction of aquatic humic acids. *Cent. Eur. J. Chem.* **2011**, *9*, 598–604. [[CrossRef](#)]
58. Geng, N.; Chen, W.; Xu, H.; Ding, M.; Liu, Z.; Shen, Z. A sono-photocatalyst for humic acid removal water: Operational parameters, kinetics and mechanism. *Ultrason. Sonochem.* **2019**, *57*, 242–252. [[CrossRef](#)]
59. Anirudhas, T.S.; Suchithra, P.S.; Rajith, S. Amine-modified polyacrylamide-bentonite composite for the adsorption of humic acid in aqueous solutions. *Colloid Surfaces A Physicochem. Eng. Asp.* **2008**, *326*, 147–156. [[CrossRef](#)]

60. Chen, K.; Feng, Q.; Feng, Y.; Ma, D.; Wan, D.; Liu, Z.; Zhu, W.; Li, Z.; Qin, F.; Feng, J. Ultrafast removal of humic acid by amine-modified silica aerogel: Insights from experiments and density functional theory calculation. *Chem. Eng. J.* **2022**, *435*, 135171. [[CrossRef](#)]
61. Zhang, J.; Kang, M.; Zhou, Y.; Ma, C.; Ning, F.; Qiu, Z. Facile synthesis of polyethyleneimine modified magnetic graphite: An effective adsorbent for the removal of humic acid from aqueous solution. *Mater. Chem. Phys.* **2020**, *255*, 123549. [[CrossRef](#)]
62. Naseem, S.; Aslam, Z.; Abbas, A.; Sumbal, S.; Ali, R.; Usman, M. Synthesis and application of cobalt-based metal-organic framework for adsorption of humic acid from water. *Chem. Biochem. Eng. Q.* **2022**, *36*, 39–50. [[CrossRef](#)]

Disclaimer/Publisher’s Note: The statements, opinions and data contained in all publications are solely those of the individual author(s) and contributor(s) and not of MDPI and/or the editor(s). MDPI and/or the editor(s) disclaim responsibility for any injury to people or property resulting from any ideas, methods, instructions or products referred to in the content.